

## Article

# Imaging Cataract-Specific Peptides in Human Lenses

Kevin L. Schey \*, Zhen Wang , Kristie L. Rose and David M. G. Anderson

Department of Biochemistry and Mass Spectrometry Research Center, Vanderbilt University School of Medicine, Nashville, TN 37232, USA

\* Correspondence: k.schey@vanderbilt.edu

**Abstract:** Age-related protein truncation is a common process in long-lived proteins such as proteins found in the ocular lens. Major truncation products have been reported for soluble and membrane proteins of the lens, including small peptides that can accelerate protein aggregation. However, the spatial localization of age-related protein fragments in the lens has received only limited study. Imaging mass spectrometry (IMS) is an ideal tool for examining the spatial localization of protein products in tissues. In this study we used IMS to determine the spatial localization of small crystallin fragments in aged and cataractous lenses. Consistent with previous reports, the pro-aggregatory  $\alpha$ A-crystallin 66–80 peptide as well as  $\alpha$ A-crystallin 67–80 and  $\gamma$ S-crystallin 167–178 were detected in normal lenses, but found to be increased in nuclear cataract regions. In addition, a series of  $\gamma$ S-crystallin C-terminal peptides were observed to be mainly localized to cataractous regions and barely detected in transparent lenses. Other peptides, including abundant  $\alpha$ A3-crystallin peptides were present in both normal and cataract lenses. The functional properties of these crystallin peptides remain unstudied; however, their cataract-specific localization suggests further studies are warranted.

**Keywords:** imaging mass spectrometry; ocular lens; protein degradation; cataract



**Citation:** Schey, K.L.; Wang, Z.; Rose, K.L.; Anderson, D.M.G. Imaging Cataract-Specific Peptides in Human Lenses. *Cells* **2022**, *11*, 4042. <https://doi.org/10.3390/cells11244042>

Academic Editor: Frank Lovicu

Received: 4 November 2022

Accepted: 5 December 2022

Published: 14 December 2022

**Publisher's Note:** MDPI stays neutral with regard to jurisdictional claims in published maps and institutional affiliations.



**Copyright:** © 2022 by the authors. Licensee MDPI, Basel, Switzerland. This article is an open access article distributed under the terms and conditions of the Creative Commons Attribution (CC BY) license (<https://creativecommons.org/licenses/by/4.0/>).

## 1. Introduction

Age-related nuclear cataract (ARNC) is the most common form of age-related lens opacification and is a leading cause of visual impairment [1]. Lens protein aggregation and the resulting scattering of light causes the opacification and multiple mechanisms have been proposed to lead to protein modification. Importantly, lens proteins are long-lived proteins (LLPs) and they can undergo many post-translational modifications over a lifetime that spans many decades [2–5]. Thus, the ocular lens is an ideal tissue to examine such changes given that the proteins localized in the central lens nucleus are as old as the donor. Modifications that have been characterized in aged human lenses include: deamidation, truncation, isomerization, racemization, and crosslinking [4–8]. An important aspect of lens protein modification is the specific location where such modifications occur as this information helps to decipher if modifications are age-related. Furthermore, identification of cataract-specific modifications may suggest potential cataractogenic mechanisms. Thus, spatially resolved studies are necessary to link lens age-related protein modifications to the lens nucleus and nuclear cataract.

Imaging mass spectrometry (IMS) is an imaging technology that can provide spatial localization for proteins, peptides, lipids, and metabolites with high spatial resolution [9,10]. IMS has been applied to lens tissue to define the location of lens proteins and their modified forms in human lenses as a function of age [4,11,12]. Based on these studies, lens protein truncation begins early in life and leads to highly truncated protein forms in older nuclear fiber cells. Indeed, a large number of crystallin peptides have been discovered in aged human lenses [13,14]. One peptide,  $\alpha$ A-crystallin 66–80, has been shown to induce protein aggregation [15], suggesting that age-related truncation products can have deleterious effects in the lens. Furthermore, IMS analysis of a guinea pig model of ARNC showed that protein truncation in the lens nucleus was accelerated with hyperbaric oxygen (HBO)

treatment [16]. Thus, knowledge of cataract-specific protein truncation products would inform on potentially cataractogenic properties of such peptides.

In this study, we employed IMS to image crystallin peptides in aged and cataractous human lenses. Specific peptides were reproducibly observed in nuclear cataract regions while not observed in age-matched transparent lenses. Other peptides were excluded from cataractous regions.

## 2. Materials and Methods

### 2.1. Tissue Preparation for Imaging Mass Spectrometry (IMS)

Human lenses were acquired from National Disease Research Interchange (NDRI) (Philadelphia, PA, USA), the South Carolina Lions Eye Bank (Charleston, SC, USA) or as a gift from Dr. Donita Garland (Ocular Genomics Institute at Massachusetts Eye and Ear, Harvard University, Cambridge, MA, USA). All lenses were stored at  $-80^{\circ}\text{C}$  until use. Information related to lenses used in this study can be found in the Supplemental Section S1. Each lens was sectioned equatorially to  $10\ \mu\text{m}$  thickness using a CM 3050 cryostat (Leica CM 3050S, Leica Microsystems Inc., Bannockburn, IL, USA). Tissue sections were thaw-mounted on conductive Indium-Tin-Oxide (ITO) coated slides (Delta Technologies, Loveland, CO, USA) and vacuum desiccated for 30 min. To remove lipids, the sections were washed twice with 70% ethanol for 1 min followed by washing with 100% ethanol for 1 min. The sections were then dried in a vacuum desiccator. To enable matrix-assisted laser desorption ionization (MALDI), tissue sections were spray-coated with 2,5-dihydroxybenzoic acid (DHB) matrix (20 mg/mL in 70% ACN containing 0.1% TFA) using a TM sprayer (HTX Technologies, LLC, Carrboro, NC, USA). The TM Sprayer was operated using the following settings: flow rate 0.1 mL/min, nozzle velocity of 700 mm/min, nozzle temperature at  $85^{\circ}\text{C}$ , track spacing at 3 mm, number of passes of 8 and nitrogen pressure 9.5 psi. After matrix application, tissue sections were rehydrated at  $85^{\circ}\text{C}$  for 3 min in a sealed chamber containing 50  $\mu\text{L}$  of 50 mM acetic acid.

### 2.2. MALDI Data Acquisition

MALDI imaging mass spectrometry experiments were performed using a Bruker Rapiflex TissueTyper (Bruker Daltonics, Billerica, MA, USA) equipped with a Smartbeam 3D 10 kHz 355 nm Nd:YAG laser<sup>TM</sup> 3D laser.  $m/z$  calibration was accomplished via a linear external calibration using a mix of bovine insulin, equine cytochrome c, bovine ubiquitin I, and equine myoglobin (Bruker Daltonik, Billerica, MA, USA). Mass spectrometric analyses were performed in the linear, positive ionization mode over a mass-to-charge ( $m/z$ ) range of  $m/z$  1200 to  $m/z$  20,000. The ionization laser was scanned across the tissue surface with a raster step size of  $60\ \mu\text{m}$  and spectra from 2000 laser shots per pixel (tissue position) were averaged to produce a spectrum. Low molecular weight crystallin fragments were also analyzed in a positive ion reflector MS mode, to improve mass resolution, over an  $m/z$  range of  $m/z$  950 to  $m/z$  5000 and with a laser raster step size of  $150\ \mu\text{m}$ . Spectra from 500 laser shots were used to produce an average spectrum. The mass spectrometer was calibrated with a peptide mixture (Leu-enkephalin, Angiotensin II, Fibrinopeptide B, ACTH fragment (1–24), and insulin chain B). Ion images were generated using FlexImaging software (Version 4.1, Bruker Daltonics, Billerica, MA, USA) using RMS normalization.

To measure the accurate masses of the signals observed in IMS data in the cortex and nucleus regions, tissue from the cortex (within  $400\ \mu\text{m}$  from the capsule) and inner nucleus region (within  $500\ \mu\text{m}$  from the center) of a 55 Y.O. (C\_5\_1) cataract lens and the cortex region of 54 Y.O. (N\_5\_1) normal transparent lens was captured by laser capture microdissection (LCM). The LCM procedure was conducted using a PALM UV Laser MicroBeam laser capture microdissection system (Carl-Zeiss, Oberkochen, Germany) on tissue sections of  $12\ \mu\text{m}$  thickness on glass slides. The capture was done using a laser pressure catapulting (LPC) method and 37% laser energy. An area of roughly  $1\ \text{mm}^2$  was collected for each sample. The samples were collected in 20  $\mu\text{L}$  of water and mixed with acetonitrile containing 2% TFA to final acetonitrile concentration of 5% and loaded on C18

SpinTips (Thermo Scientific, Rockford, IL, USA). The samples were washed with 0.1%TFA and eluted in 2.5  $\mu$ L of 70% acetonitrile containing 0.1%TFA. The samples were mixed with 2.5  $\mu$ L of saturated  $\alpha$ -cyano-4-hydroxycinnamic acid (CHCA) matrix (Sigma-Aldrich, St Louis, MO, USA) in 70% acetonitrile (0.1%TFA) and masses were measured with high accuracy (<5 ppm) in a Bruker Solarix 15T FT-ICR mass spectrometer (Bruker Daltonics, Billerica, MA, USA) equipped with a Smartbeam II 2 kHz Nd:YAG (355 nm) laser. The mass spectrometer was externally calibrated prior to analysis using a peptide mixture (Leu-enkephalin, Angiotensin II, Fibrinopeptide B, ACTH fragment (1–24), and insulin chain B). The mass spectrometer was operated in positive ion mode and data were collected from  $m/z$  700 to 4500 at a mass resolution of  $\sim$ 155,000 at  $m/z = 2360.2393$ .

### 2.3. Peptide Identification and LC-MS/MS Analysis

To identify the peptides that correspond to the low molecular weight signals in MALDI imaging results, peptides were extracted from the nucleus region of two cataract lenses using 20% acetonitrile, 80% water as described previously [17]. The samples were diluted using 0.1% formic acid to reduce the acetonitrile concentration to 3% and loaded onto a C18 trap column (50 mm  $\times$  150  $\mu$ m) packed with Phenomenex Jupiter resin (5  $\mu$ m mean particle size, 300  $\text{\AA}$  pore size). The trap column was connected with a fused silica capillary analytical column (150 mm  $\times$  100  $\mu$ m) packed with Phenomenex Jupiter resin (3  $\mu$ m mean particle size, 300  $\text{\AA}$  pore size). Peptides were analyzed by LC-MS/MS on a LTQ Orbitrap Velos (Thermo Scientific, San Jose, CA, USA) mass spectrometer coupled to an Eksigent NanoLC system. Mobile phase solvents consisted of 0.1% formic acid in water (solvent A) and 0.1% formic acid in acetonitrile (solvent B). Peptides were gradient eluted at a flow rate of 500 nL/min using the following gradient: 2–45%B in 40 min; 45–90%B in 15 min; 90%B for 2 min; 90–2%B in 1 min; and 2%B for 15 min (column equilibration). Peptides were introduced into the LTQ Orbitrap Velos using a nanoelectrospray source. The instrument was operated using a combined method consisting of both data-dependent electron transfer dissociation (ETD) and targeted ETD scan events. MS1 acquisition was performed in the Orbitrap ( $R = 60,000$ ) with an AGC target value of  $1e6$ . The MSn AGC target value of  $9e5$  was used in the Orbitrap and  $2e4$  in the ion trap. Dynamic exclusion (repeat count 1, exclusion list size 500, and exclusion duration 15 s) was enabled. For ETD, an isolation width of 3  $m/z$  and reaction time of 80 ms were used. The ETD reagent ion AGC target was  $3e6$ . ETD MS/MS spectra were interpreted manually.

## 3. Results

### 3.1. Detection of Low Molecular Signals in Cataract Nucleus

In this study, an untargeted approach using imaging mass spectrometry (IMS) was used to examine protein degradation in different regions of normal and cataract human lenses. In addition to intact crystallins and longer truncated crystallin fragments reported previously [9], IMS analysis also revealed lower molecular weight (LMW) signals and some of these signals were only detected in the nucleus region of nuclear cataract lenses. A typical IMS result is shown in Figure 1, which shows the presence of signals at  $m/z$  2933 and 4098 in the nucleus of the two cataract lenses (55 Y.O. (C\_5\_1) and 56 Y.O. (C\_5\_2)). These two signals were not present in the nucleus of a 54 Y.O. (N\_5\_1) normal transparent lens.

Note that Figure 1 also showed the presence of a signal at  $m/z$  2933 in the cortex of both normal and cataract lenses. Due to absence of this signal in the inner cortex and outer nucleus region, we hypothesized that the signal in the cortex could represent a different peptide with similar molecular weight to the one in the nucleus. Due to the low mass resolving power of the linear MALDI-TOF instrument used in this experiment, two molecules with close molecular weights, i.e., nominal isobars, could not be mass resolved. To test this hypothesis, tissues from the cortex and nucleus regions were collected by LCM and the samples were analyzed using a high mass resolution FT-ICR mass spectrometer. The results shown in Figure 2 confirmed our hypothesis. The protonated ion in the 54 Y.O.(N\_5\_1) cortex region has measured  $m/z$  value of 2930.4939 and the measured  $m/z$

value in 55 Y.O. (C\_5\_1) cataract lens cortex was 2930.4999, but the signal in the nucleus region has measured  $m/z$  value of 2931.6001. This result confirmed the 2933 signal in the cortex region shown Figure 1 corresponds to a different peptide from the signal in the cataract nucleus. The signal at  $m/z$  2930.4939 in the lens cortex has not been identified in subsequent LC-MS/MS experiments of nuclear extracts; however, the mass matches a  $\beta$ B2-crystallin 182–205 peptide with a mass error 4.2 ppm and this  $\beta$ B2-crystallin peptide was previously reported to be present in human lenses [13].

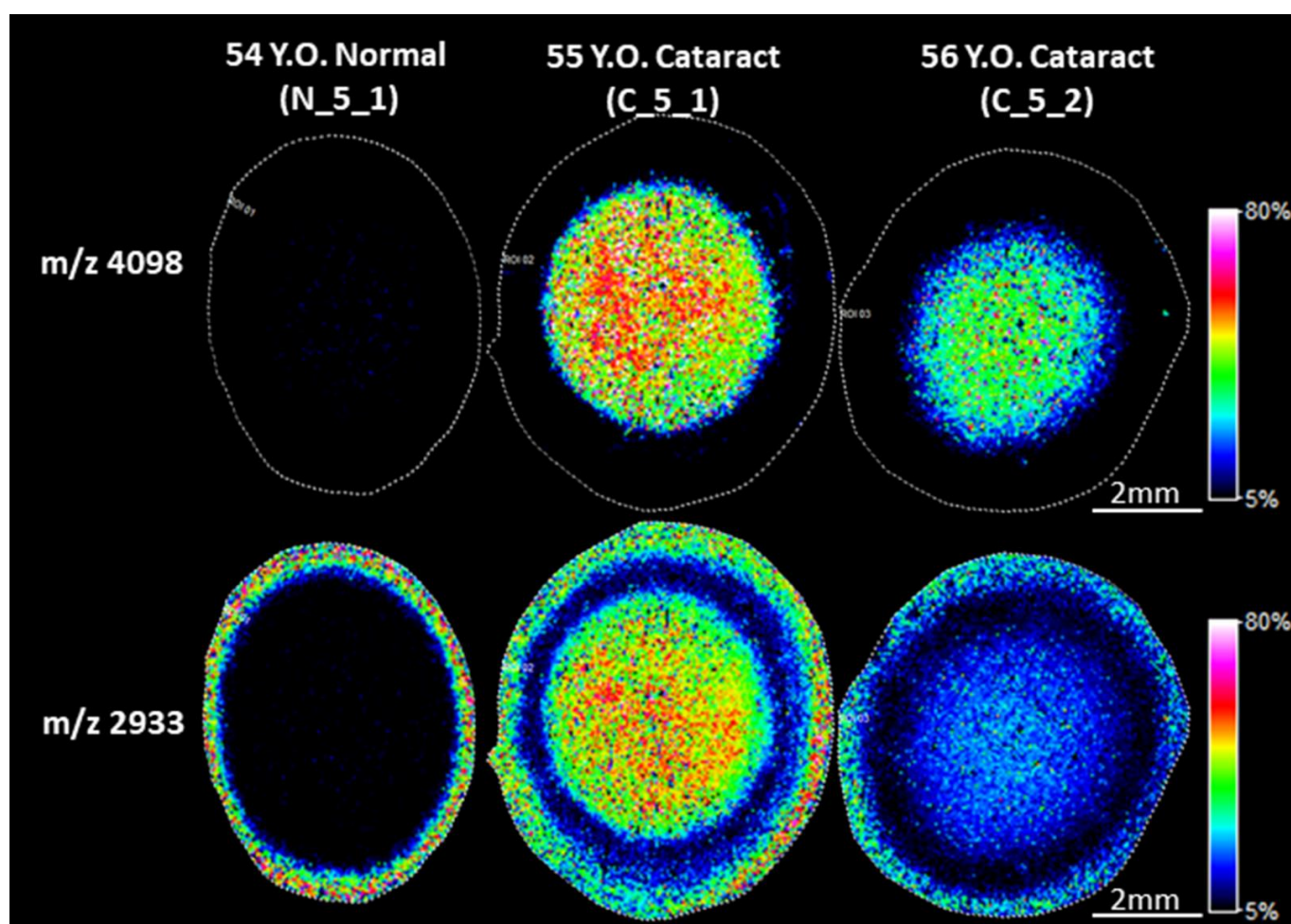


**Figure 1.** Cataract-specific signals in the nucleus of cataract lenses. Imaging mass spectrometry (IMS) analysis of human lens sections was performed on Bruker Rapiflex Tissuetyper using a 60  $\mu$ m raster step size. IMS analysis identified two signals with  $m/z$  values of 4098 and 2933 that were only detected in the nucleus of cataract lenses, but not in normal lens nucleus. Accurate mass measurement confirmed  $m/z$  2933 signal in the cortex region represent a different peptide than that represented by the signal in the cataract nucleus. Signal represents peak  $m/z$  value  $\pm$  0.1%  $m/z$  unit.

### 3.2. Identification of Signals Detected by IMS and Further Confirmation of Cataract Specificity

Identification of the peptides at  $m/z$  2933 and 4098 was performed based on their accurate masses and their tandem mass spectra in LC-MS/MS experiments. To identify these signals, a 20% acetonitrile extract from the nucleus region of a 70 Y.O. (C\_7\_1) cataract lens was analyzed by LC-MS/MS. The base peak chromatogram from the LC-MS/MS analysis is shown in Figure 3 which further confirms the presence of two abundant signals with the measured mass of a protonated ion ( $[MH]^+$ ) of 2931.5942 and 4096.1988. These measured masses match  $\gamma$ S-crystallin peptide sequences 154–178 and 145–178, respectively, within 1 ppm mass accuracy. Their identifications were further confirmed by their tandem mass spectra. The ETD tandem mass spectrum of  $\gamma$ S-crystallin peptide 154–178 (+4 ion)

is shown in Figure 4A displaying excellent matches to the peptide sequence with a series of c and z ions. The tandem mass spectrum for  $\gamma$ S-crystallin peptide 145–178 (+6 ion) can be found in Figure 4B. In addition to these two  $\gamma$ S peptide signals, manual analysis of the major LC-MS/MS signals confirmed the presence of multiple  $\gamma$ S-crystallin,  $\beta$ A3-crystallin and  $\gamma$ D-crystallin C-terminal peptides in the cataract lens nucleus sample. These signals are labeled in the base peak chromatogram (Figure 3). A list of these peptides with their measured and predicted masses is shown in Table 1.

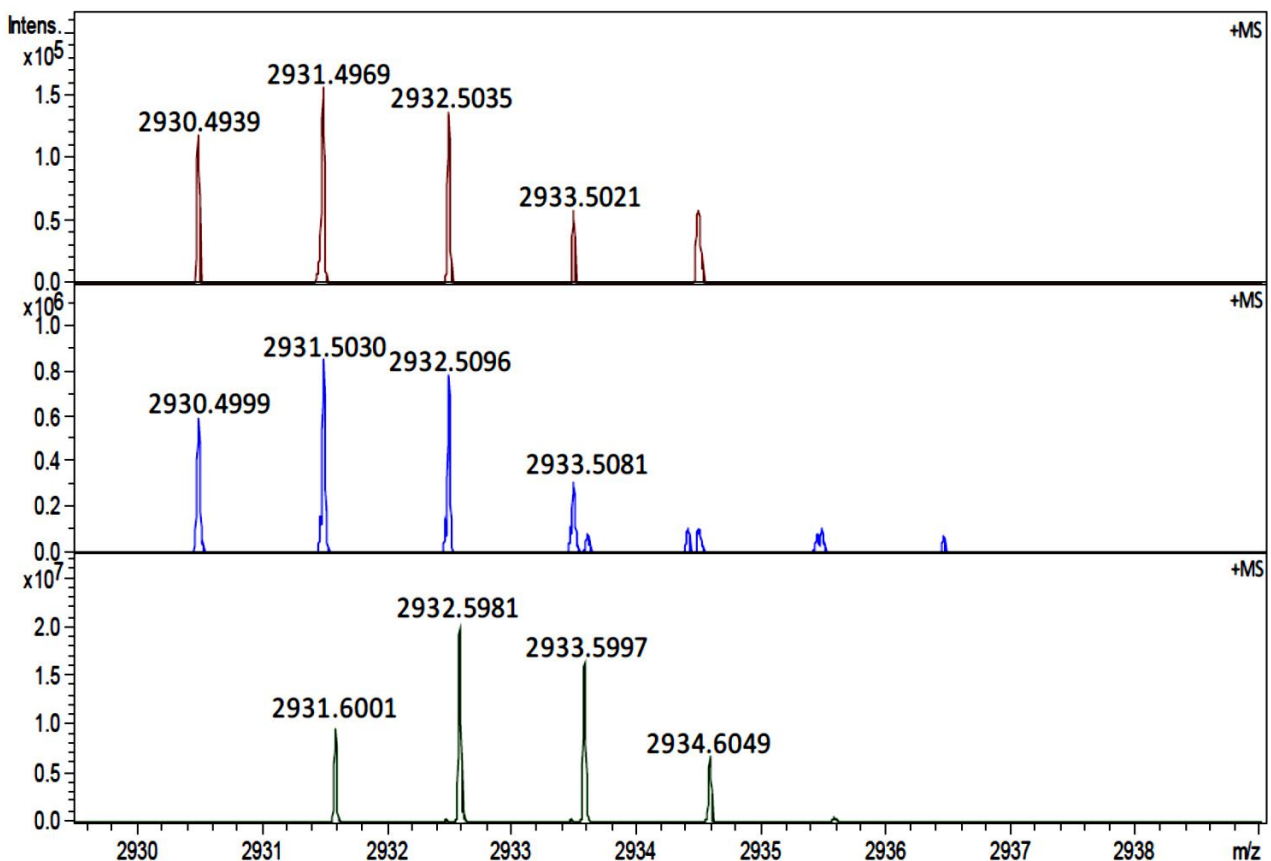


**Figure 2.** Accurate mass measurement of the signal at  $m/z$  2933 in cortex and nucleus regions using an FT-ICR mass spectrometer. The positive mode mass spectra from LCM captured cortex and nucleus samples were zoomed in to show the isotopic distribution of signals at  $m/z$  2933. The protonated ion in a 54 Y.O. (N\_5\_1) normal lens cortex region (**top row**) has a measured monoisotopic mass of 2930.4939 Da and 2930.4999 Da in 55 Y.O. (C\_5\_1) cataract lens cortex (**middle row**), but has a measured monoisotopic mass of 2931.6001 Da in 55 Y.O. cataract lens nucleus (**bottom row**).

To further confirm whether  $\gamma$ S-crystallin peptides 154–178 and 145–178 are indeed cataract-specific, several IMS datasets were acquired from multiple human lenses. The data are shown in Figure S1. The results from multiple datasets, acquired on different instruments and using different experimental conditions, consistently confirmed the presence of  $\gamma$ S-crystallin 154–178 and  $\gamma$ S-crystallin 145–178 in cataract lens nuclei, but not in normal lenses. A weak signal of  $\gamma$ S-crystallin 145–178 can sometimes be detected in aged normal lens (70 Y.O. (N\_7\_1) and 78 Y.O. (N\_7\_2)), but the signal intensity of this peptide was significantly stronger in age-matched cataract lens nuclei. Moreover, a mild nuclear cataract could have been missed in the evaluation of these aged lenses.

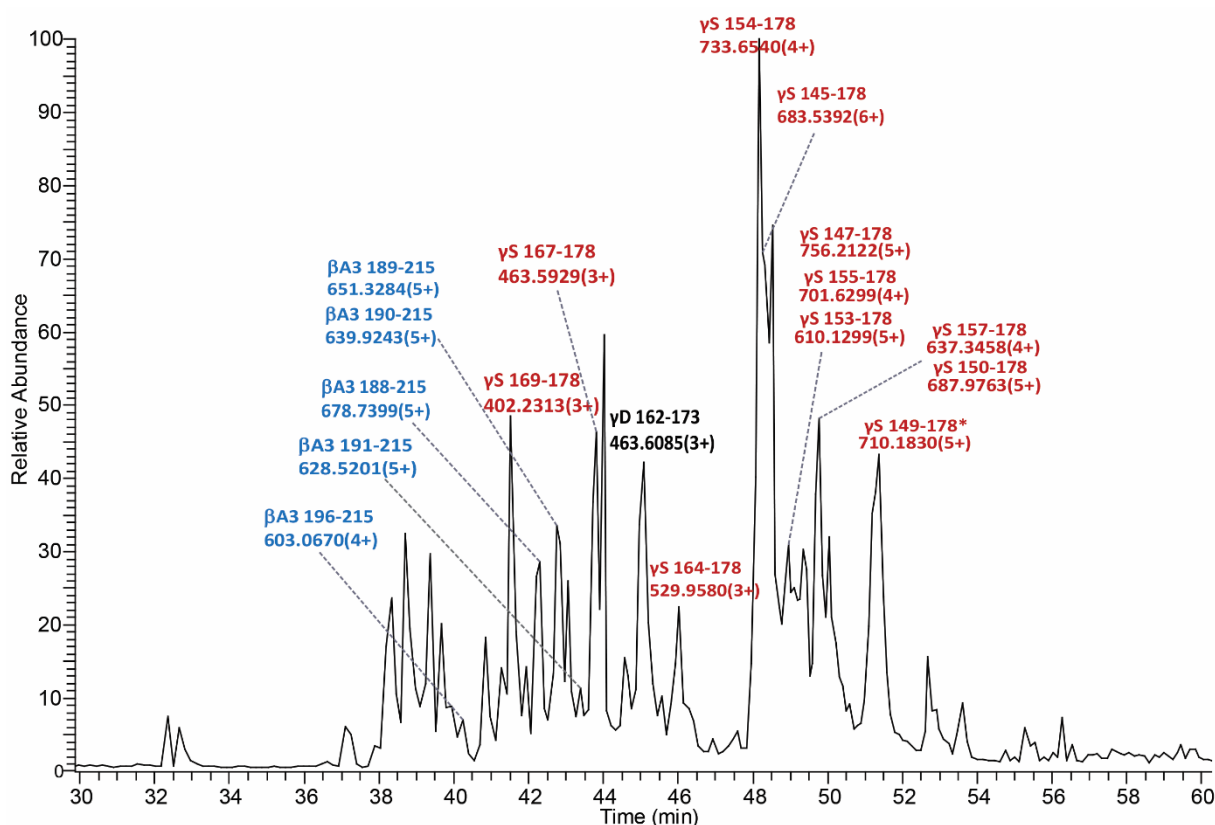


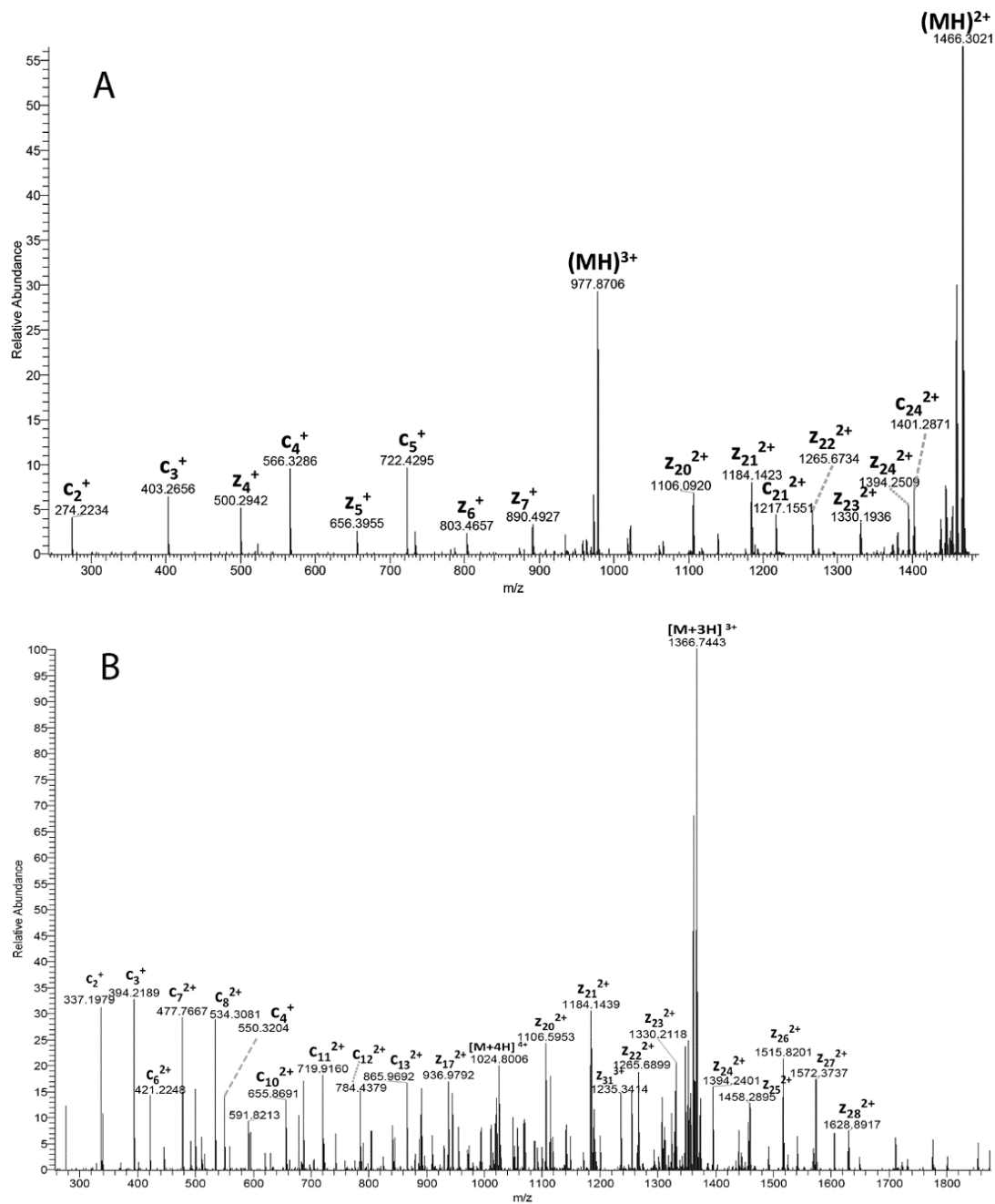
**Figure 3.** The base peak chromatogram of LC-MS/MS analysis of the extract from a 70 Y.O. (C\_7\_1) nucleus of a cataract lens. The base peak chromatogram is dominated by strong signals of  $\gamma$ S- and  $\beta$ A3-crystallin fragments. Two strongest signals are identified as  $\gamma$ S154–178 and  $\gamma$ S145–178. Other base peak signals were identified as  $\gamma$ S-crystallin C-terminal peptides (red),  $\beta$ A3-crystallin C-terminal peptides (blue) and a  $\gamma$ D-crystallin C-terminal peptide (black). \* indicates pyroGlu at the N-terminus.

IMS data were also acquired in a low mass range using a higher mass resolution reflector MALDI-TOF instrument. The results can be found in Figure 5. Consistent with aforementioned results,  $\gamma$ S-crystallin 154–178 and  $\gamma$ S-crystallin 145–178 were detected in cataract nuclei, but not in cataract cortex and normal lenses. Other than  $\gamma$ S-crystallin 145–178 and  $\gamma$ S-crystallin 154–178, other signals that were highly abundant in the cataract nucleus compared to cortex tissue in cataract and normal lenses were also detected (Figure 5). The signal at  $m/z$  1204 was identified as  $\gamma$ S-crystallin 169–178. Other signals at  $m/z$  1849 and  $m/z$  1779 correspond to  $\alpha$ A-crystallin 66–80 and  $\alpha$ A-crystallin 67–80, respectively. Consistent with previous reports [13,14,18], a weak signal of  $\alpha$ A 66–80 and 67–80 was detected in the normal lens, but intensities of these peptides were significantly higher in the cataract lenses. The accurate mass measurement again showed the signal at nominal  $m/z$  1389 corresponds to two peptides  $\gamma$ S-crystallin 167–178 and  $\gamma$ D-crystallin 162–173. As shown in Figure S2, the signal in the cortex was mainly from  $\gamma$ S-crystallin 167–178 (calculated  $m/z$  1388.7645), but in the nucleus, intensities of both  $\gamma$ S-crystallin 167–178 and  $\gamma$ D-crystallin 162–173 (calculated  $m/z$  1388.8121) were similar. Therefore, both peptides contribute roughly equally to the signal at  $m/z$  1389 in the nucleus. The weak signal of  $\gamma$ S-crystallin 167–178 in normal lens and cataract lens cortex was also consistent with previous reports [13,14,19].

### 3.3. Low Molecular Weight Signals in Normal Lenses

As shown in Figure 3, some strong LMW signals are identified as  $\beta$ A3-crystallin peptides. Unlike  $\gamma$ S-crystallin peptides, IMS analysis showed  $\beta$ A3-crystallin peptides were detected in both normal and cataract lenses. IMS results from three middle-aged lenses are shown in Figure 6. These results suggest that  $\beta$ A3-crystallin undergoes degradation

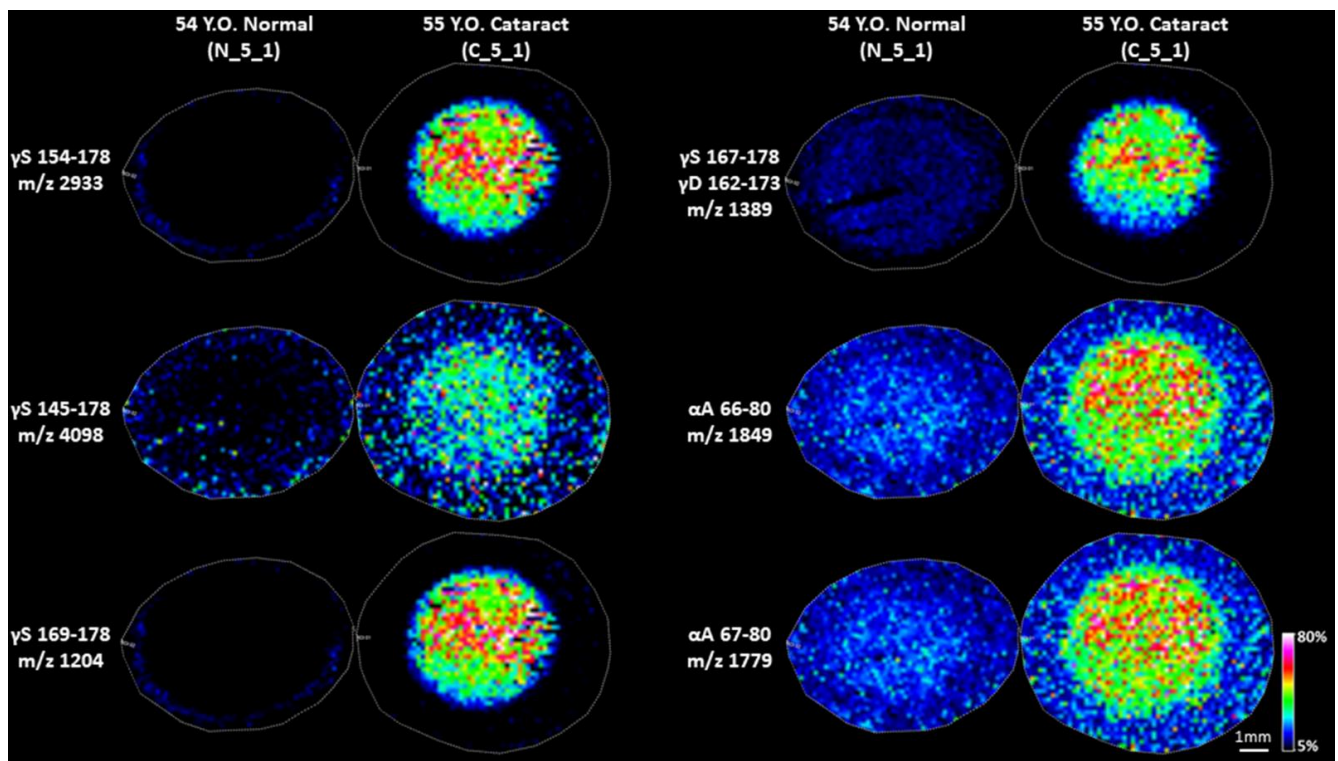
and this process starts earlier than  $\gamma$ S-crystallin degradation since strong signals from  $\beta$ A3-crystallin 188–215 and  $\beta$ A3-crystallin 189–215 can be detected in the cortical fiber cells of the middle-aged lenses. Signals from  $\beta$ A3-crystallin fragments did not show a difference between normal lens cortex and cataract lens cortex, however, signals from the longer peptides, especially  $\beta$ A3-crystallin 188–215, dramatically decreased and the signal from the shorter fragments ( $\beta$ A3-crystallin 191–215 and 192–215) significantly increased in the nucleus of the cataract lenses. The longest  $\beta$ A3-crystallin C-terminal peptide detected was 187–215 and shorter peptides were detected corresponding to removal of residues from the new N-terminus. These results suggest that initial cleavage occurs at the Asp186-His187 peptide bond, that further degradation of peptide products continues with age, and that this process is elevated in the cataract nucleus.



**Figure 4.** ETD tandem mass spectra of: (A)  $\gamma$ S-crystallin 154–178 (+4 charged ion) and (B)  $\gamma$ S-crystallin 145–178 (+6 charged ion). All masses labeled represent the monoisotopic masses.

**Table 1.** Identified major  $\gamma$ S-,  $\gamma$ D- and  $\beta$ A3-crystallin peptides in the nucleus of a 70 Y.O. (C\_7\_1) cataract lens.

Protein	Predicted $m/z$ <sup>a</sup>	Observed $m/z$	Error (ppm)
Gamma S 145–178	4096.1992	4096.1988	0.1
Gamma S 147–178	3777.0347	3777.0319	0.74
Gamma S 149–178 (pyroGlu)	3546.8856	3546.8859	0.1
Gamma S 150–178	3435.8536	3435.8524	0.35
Gamma S 153–178	3046.6221	3046.6204	0.56
Gamma S 154–178	2931.5952	2931.5942	0.35
Gamma S 155–178	2803.5002	2803.4978	0.87
Gamma S 157–178	2546.3627	2546.3614	0.52
Gamma S 164–178	1587.8602	1587.8594	0.47
Gamma S 167–178	1388.7645	1388.7641	0.25
Gamma S 169–178	1204.6797	1204.6793	0.29
Beta A3 188–215	3389.6747	3389.6704	1.3
Beta A3 189–215	3252.6158	3252.6129	0.89
Beta A3 190–215	3195.5943	3195.5924	0.6
Beta A3 191–215	3138.5729	3138.5714	0.5
Beta A3 196–215	2409.2494	2409.2462	1.3
Gamma D 162–173	1388.8121	1388.8109	0.83

<sup>a</sup> monoisotopic  $m/z$ .**Figure 5.** IMS images of LMW fragments specific or highly enriched in cataract lenses. Images were acquired on Bruker Rapiflex Tissue typer using a 150  $\mu$ m raster step size. Signal represents peak  $m/z$  value  $\pm$  0.01%  $m/z$  unit.

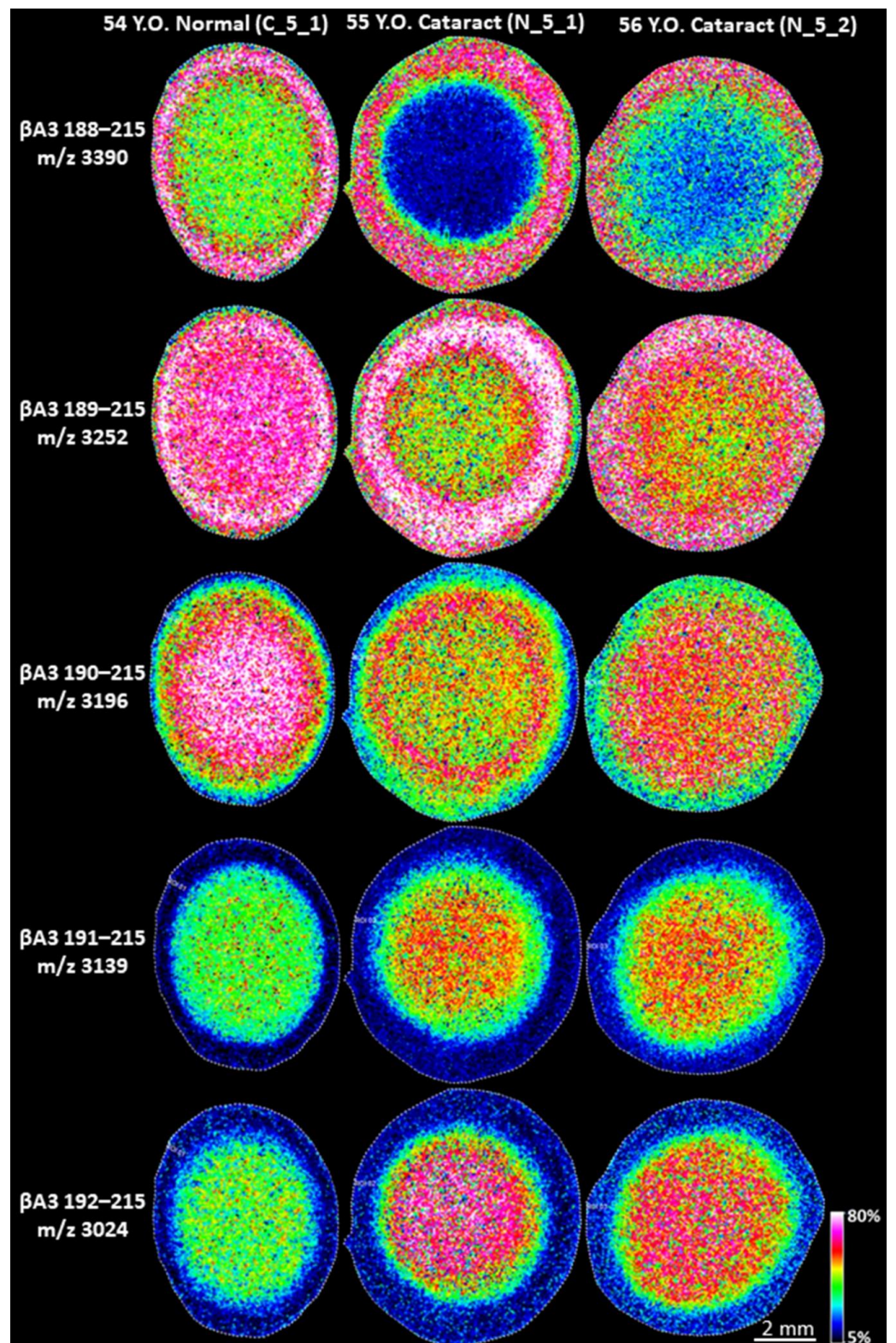


**Figure 6.** IMS analysis of  $\beta$ A3 peptides in normal and cataract lenses. IMS analysis of human lens sections was performed on Bruker Rapiflex Tissue typer using a 60  $\mu$ m raster step size. Multiple  $\beta$ A3-crystallin fragments were detected in normal and cataract lenses. The protein cleavage started in lens cortex and  $\beta$ A3 fragments were further degraded and their formation was accelerated in cataract lens nuclei. Signal represents peak  $m/z$  value  $\pm$  0.1%  $m/z$  unit.

#### 4. Discussion

Accumulation of low molecular weight (LMW) crystallin fragments in aged and cataract lenses has been characterized by multiple investigators [12–14,17,18] and some major crystallin fragments, including peptides from  $\alpha$ A-,  $\alpha$ B- and  $\beta$ A3-crystallins [13–15,18], have been repeatedly reported. However, with the exception of  $\gamma$ S-crystallin 167–178 and 2–22 peptides, other  $\gamma$ S-crystallin LMW peptides have not been reported. In this study, we identify LMW peptides from the  $\gamma$ S-crystallin C-terminus as the dominating signals in the nucleus region of nuclear cataract lenses. Most noteworthy, these LMW fragments are cataract-specific since they were either not detected or were of very low abundance in normal lenses by IMS. One might ask why these abundant  $\gamma$ S-crystallin peptides in cataract lens nucleus were not detected previously [13,14]. We speculate that the reason is due to the strong membrane binding and hydrophobic properties of these peptides. As previously suggested,  $\gamma$ S-crystallin 167–178 can only be extracted from the membrane with NaOH or ethanol [18]. Thus, the peptides reported in this study are likely to be strongly bound to fiber cell membranes. In fact, the  $\gamma$ S-crystallin 167–178 peptide has been reported to strongly bind to the cell membrane and may also affect water permeability [18]. Thus, the hydrophobic properties of C-terminal  $\gamma$ S-crystallin peptides could induce protein aggregation and/or plasma membrane binding.

$\gamma$ S-crystallin, formerly known as  $\beta$ S-crystallin, belongs to the  $\beta\gamma$ -crystallin superfamily of lens crystallins. Based on sequence homology and predicted tertiary structure,  $\gamma$ S-crystallin was found to be more closely related to the monomeric  $\gamma$ -crystallins than to the oligomeric  $\beta$ -crystallins and its name was changed to  $\gamma$ S-crystallin [20].  $\gamma$ S-Crystallin is synthesized postnatally and is highly abundant in the ocular lens [21], whereas other  $\gamma$ -crystallins are primarily synthesized before birth and are mainly present in the lens nucleus [21]. Multiple single-residue mutations in  $\gamma$ S-crystallin were reported to be associated with formation of different types of cataract [22]. Deamidation of Asn76 in  $\gamma$ S-crystallin was found in greater abundance in cataract lenses compared to normal lenses [7]. The finding of the LMW  $\gamma$ S-crystallin peptides to be specifically present in the nucleus of nuclear cataract lenses further supports the importance of  $\gamma$ S-crystallin during cataractogenesis. Consistent with our results, it was reported that the monomeric full length of  $\gamma$ S-crystallin was diminished in nuclear cataract lenses [23]. Clearly, extensive degradation of  $\gamma$ S-crystallin occurs in nuclear cataract. How the properties of the observed C-terminal fragments contribute to opacification remains to be elucidated.

Our finding of cataract-specific LMW fragments in nuclear cataracts support the hypothesis that the development of cataract is due, at least in part, to the aggregation of crystallin fragments generated by the breakdown of crystallin proteins [15,24]. The discovery of a LMW  $\alpha$ A-crystallin peptide, residues 66–80, that induced protein aggregation and light scattering as well as caused loss of  $\alpha$ -crystallin chaperone activity [15] also supports this hypothesis [13,15]. We observed this specific  $\alpha$ A-crystallin peptide in cataractous lens nuclei along with  $\alpha$ A-crystallin 67–80. In addition to LMW peptides, truncated crystallins have been found to be more prone to aggregation [18].

Considering the potential protein aggregation properties of the LMW fragments, it is important to understand the mechanisms that mediate the cleavage of crystallins. No protease has been linked with previously reported LMW peptides [13,14]. Human  $\beta$ A3-crystallin was reported to possess autodegradative serine protease activity that could be responsible for degradation of the  $\beta$ A3-crystallin N-terminus (Gln4-Ala5 and Lys17-Met18) [25], however, this would not explain the formation of the  $\beta$ A3-crystallin C-terminal fragments. The longest  $\beta$ A3-crystallin C-terminal fragment is  $\beta$ A3-crystallin 187–215 corresponding to cleavage at Asp186. We believe the peptide 187–215 is formed first followed by further removal of residues from the N-terminus resulting in multiple peptides with different lengths. Our IMS results also confirm that the formation of  $\beta$ A3-crystallin peptides starts in young cortical fiber cells and the peptides formed were further degraded in the nucleus. Similarly, the formation of  $\gamma$ D-crystallin 162–173 corresponds to cleavage at Asn 161. Spontaneous cleavage at Asp and Asn through a succinimide intermediate [26] or

Glu or Gln through a glutarimide [27] is a well-known mechanism for protein cleavage and this process is also coupled with deamidation, isomerization, and racemization of Asn or Gln residues [26]. These mechanisms explain truncation, deamidation and isomerization at many different Asn, Asp, Gln and Glu residues throughout the lens proteome, especially the ones that are followed by small, flexible residues such as glycine [26,28,29]. Another spontaneous cleavage mechanism, i.e., cleavage on the N-terminal side of Ser that may involve an intein-like mechanism [19,30] could be responsible for the formation of  $\gamma$ S-crystallin 167–178. Both proposed mechanisms are expected to occur in both normal and cataract lenses and, correspondingly, predicted LMW peptides can be detected in both normal and cataract lenses.

The two major cataract-specific  $\gamma$ S-crystallin peptides detected in this study are produced by cleavage after Asn144 and Asp153. Therefore, similar to other lens peptides, spontaneous cleavage through a succinimide intermediate could also contribute to the formation of these peptides. Additional removal of N-terminus residues generates other shorter  $\gamma$ S-crystallin peptides detected in nucleus of cataract lenses. However, the succinimide mechanism is a common mechanism that is responsible for the most prevalent modifications such as deamidation and isomerization in aged normal lenses [4,8,31]. It is questionable why these  $\gamma$ S-crystallin peptides were only detected in cataract lens nuclei if a common aging mechanism is responsible for the formation of these peptides. In addition, succinimide mediated deamidation and truncation is characterized by formation of multiple isomers after deamidation and truncation. From our LC-MS/MS analysis of trypsin digested human lens samples, multiple isomers can be detected for the  $\beta$ A3-crystallin 178–193 (containing Asp186) and  $\gamma$ D-crystallin 154–163 (containing Asn161); however, the  $\gamma$ S-crystallin peptide 132–146 (plus deamidation) and 149–154 were present as single peaks indicating lack of isomerization (data not shown). Even though cleavage at Asn144 and Asp153 in  $\gamma$ S-crystallin occurs at Asp and Asn residues, this cleavage may be through a different mechanism other than through a succinimide intermediate. Another possible explanation is that LMW peptides formed in normal lenses can be effectively degraded, but this degradation process is lost in cataract lenses resulting in accumulation of these peptides. Further study is needed to understand the mechanism for formation and accumulation of LMW  $\gamma$ S-crystallin fragments in cataract lenses.

**Supplementary Materials:** The following supporting information can be downloaded at: <https://www.mdpi.com/article/10.3390/cells11244042/s1>, Figure S1: IMS analysis of  $\gamma$ S 145–178 and  $\gamma$ S 154–178 in normal and cataract lenses; Figure S2: The accurate mass measurement of the signal at  $m/z$  1389; Section S1.

**Author Contributions:** K.L.S. & Z.W. wrote the manuscript. K.L.S., Z.W., D.M.G.A. & K.L.R. were involved in the planning of experiments, acquiring data, and editing the manuscript. All authors have read and agreed to the published version of the manuscript.

**Funding:** This research was funded by National Institutes of Health grant number R01 EY013462 and P30 EY008126.

**Data Availability Statement:** The raw data is available on request that should be send to [k.schey@vanderbilt.edu](mailto:k.schey@vanderbilt.edu).

**Acknowledgments:** The authors acknowledge Donita Garland of the Ocular Genomics Institute at Massachusetts Eye and Ear, Harvard Medical School for providing some nuclear cataract lenses. The authors also acknowledge the funding support by National Institutes of Health by grants R01 EY013462 and P30 EY008126 and the use of Proteomics and Tissue Imaging Core Facility of the Vanderbilt University Mass Spectrometry Research Center.

**Conflicts of Interest:** The authors have no potential conflict of interest to declare.

## References

1. Congdon, N.; Vingerling, J.R.; Klein, B.E.K.; West, S.; Friedman, D.; Kempen, J.; O'Colmain, B.; Wu, S.-Y.; Taylor, H.R. Eye Diseases Prevalence Research Group Prevalence of Cataract and Pseudophakia/Aphakia Among Adults in the United States. *Arch. Ophthalmol.* **2004**, *122*, 487–494. [[CrossRef](#)] [[PubMed](#)]
2. Truscott, R.J.; Schey, K.L.; Friedrich, M.G. Old Proteins in Man: A Field in its Infancy. *Trends Biochem. Sci.* **2016**, *41*, 654–664. [[CrossRef](#)] [[PubMed](#)]
3. Takemoto, L. Quantitation of C-terminal modification of alpha-A crystallin during aging of the human lens. *Exp. Eye Res.* **1995**, *60*, 721–724. [[PubMed](#)]
4. Wilmarth, P.A.; Tanner, S.; Dasari, S.; Nagalla, S.R.; Riviere, A.; Bafna, V.; Pevzner, P.A.; David, L.L. Age-related changes in human crystallins determined from comparative analysis of post-translational modifications in young and aged lens: Does deamidation contribute to crystallin insolubility? *J. Proteome Res.* **2006**, *5*, 2554–2566. [[CrossRef](#)] [[PubMed](#)]
5. Grey, A.C.; Schey, K.L. Age-Related Changes in the Spatial Distribution of Human Lens  $\alpha$ -Crystallin Products by MALDI Imaging Mass Spectrometry. *Investig. Ophthalmology Vis. Sci.* **2009**, *50*, 4319–4329. [[CrossRef](#)] [[PubMed](#)]
6. Takemoto, L.; Boyle, D. Increased deamidation of asparagine during human senile cataractogenesis. *Mol. Vis.* **2000**, *6*, 164–168.
7. Hooi, M.Y.; Rafferty, M.J.; Truscott, R.J. Racemization of two proteins over our lifespan: Deamidation of asparagine 76 in gammaS crystallin is greater in cataract than in normal lenses across the age range. *Investig. Ophthalmol. Vis. Sci.* **2012**, *53*, 3554–3561. [[CrossRef](#)]
8. Lyon, Y.A.; Sabbah, G.M.; Julian, R.R. Differences in  $\alpha$ -crystallin isomerization reveal the activity of protein isoaspartyl methyltransferase (PIMT) in the nucleus and cortex of human lenses. *Exp. Eye Res.* **2018**, *171*, 131–141. [[CrossRef](#)]
9. Seeley, E.H.; Caprioli, R.M. Molecular imaging of proteins in tissues by mass spectrometry. *Proc. Natl. Acad. Sci. USA* **2008**, *105*, 18126–18131. [[CrossRef](#)]
10. Buchberger, A.R.; Delaney, K.; Johnson, J.; Jillian, J. Mass Spectrometry Imaging: A Review of Emerging Advancements and Future Insights. *Anal. Chem.* **2017**, *90*, 240–265. [[CrossRef](#)]
11. Wenke, J.L.; Rose, K.L.; Spraggins, J.M.; Schey, K.L. MALDI Imaging Mass Spectrometry Spatially Maps Age-Related Deamidation and Truncation of Human Lens Aquaporin-0. *Investig. Ophthalmol. Vis. Sci.* **2015**, *56*, 7398–7405. [[CrossRef](#)] [[PubMed](#)]
12. Anderson, D.M.; Nye-Wood, M.G.; Rose, K.L.; Donaldson, P.J.; Grey, A.C.; Schey, K.L. MALDI imaging mass spectrometry of  $\beta$ - and  $\gamma$ -crystallins in the ocular lens. *J. Mass Spectrom.* **2020**, *55*, e4473. [[CrossRef](#)] [[PubMed](#)]
13. Santhoshkumar, P.; Udupa, P.; Murugesan, R.; Sharma, K.K. Significance of Interactions of Low Molecular Weight Crystallin Fragments in Lens Aging and Cataract Formation. *J. Biol. Chem.* **2008**, *283*, 8477–8485. [[CrossRef](#)]
14. Su, S.-P.; McArthur, J.D.; Aquilina, J.A. Localization of low molecular weight crystallin peptides in the aging human lens using a MALDI mass spectrometry imaging approach. *Exp. Eye Res.* **2010**, *91*, 97–103. [[CrossRef](#)] [[PubMed](#)]
15. Santhoshkumar, P.; Raju, M.; Sharma, K.K.  $\alpha$ A-crystallin peptide SDRDKFVIFLDVKHF accumulating in aging lens impairs the function of  $\alpha$ -crystallin and induces lens protein aggregation. *PLoS ONE.* **2011**, *6*, e19291. [[CrossRef](#)]
16. Giblin, F.J.; Anderson, D.M.; Han, J.; Rose, K.L.; Wang, Z.; Schey, K.L. Acceleration of age-induced proteolysis in the guinea pig lens nucleus by in vivo exposure to hyperbaric oxygen: A mass spectrometry analysis. *Exp. Eye Res.* **2021**, *210*, 108697. [[CrossRef](#)]
17. Schey, K.L.; Anderson, D.M.; Rose, K.L. Spatially-Directed Protein Identification from Tissue Sections by Top-Down LC-MS/MS with Electron Transfer Dissociation. *Anal. Chem.* **2013**, *85*, 6767–6774. [[CrossRef](#)]
18. Srivastava, O.; Srivastava, K.; Chaves, J.; Gill, A. Post-translationally modified human lens crystallin fragments show aggregation in vitro. *Biochem. Biophys. Rep.* **2017**, *10*, 94–131. [[CrossRef](#)]
19. Friedrich, M.G.; Lam, J.; Truscott, R.J. Degradation of an old human protein: Age-dependent cleavage of gammaS-crystallin generates a peptide that binds to cell membranes. *J. Biol. Chem.* **2012**, *287*, 39012–39020. [[CrossRef](#)]
20. Quax-Jeuken, Y.; Driessen, H.; Leunissen, J.; Quax, W.; de Jong, W.; Bloemendal, H. beta s-Crystallin: Structure and evolution of a distinct member of the beta gamma-superfamily. *EMBO J.* **1985**, *4*, 2597–2602. [[CrossRef](#)]
21. Thomson, J.A.; Augusteyn, R.C. Ontogeny of human lens crystallins. *Exp. Eye Res.* **1985**, *40*, 393–410. [[CrossRef](#)] [[PubMed](#)]
22. Vendra, V.P.R.; Khan, I.; Chandani, S.; Muniyandi, A.; Balasubramanian, D. Gamma crystallins of the human eye lens. *Biochim. Biophys. Acta (BBA)-Gen. Subj.* **2016**, *1860*, 333–343. [[CrossRef](#)] [[PubMed](#)]
23. Schey, K.L.; Wang, Z.; Friedrich, M.G.; Garland, D.L.; Truscott, R.J. Spatiotemporal changes in the human lens proteome: Critical insights into long-lived proteins. *Prog. Retin. Eye Res.* **2019**, *76*, 100802. [[CrossRef](#)] [[PubMed](#)]
24. David, L.L.; Shearer, T.R. Role of proteolysis in lenses: A review. *Lens. Eye Toxic. Res.* **1989**, *6*, 725–747. [[PubMed](#)]
25. Gupta, R.; Chen, J.; Srivastava, O.P. A serine-type protease activity of human lens betaA3-crystallin is responsible for its auto-degradation. *Mol. Vis.* **2010**, *16*, 2242–2252. [[PubMed](#)]
26. Voorter, C.E.; de Haard-Hoekman, W.A.; Oetelaar, P.J.V.D.; Bloemendal, H.; De Jong, W.W. Spontaneous peptide bond cleavage in aging alpha-crystallin through a succinimide intermediate. *J. Biol. Chem.* **1988**, *263*, 19020–19023. [[CrossRef](#)]
27. Friedrich, M.G.; Wang, Z.; Schey, K.L.; Truscott, R.J.W. Spontaneous Cleavage at Glu and Gln Residues in Long-Lived Proteins. *ACS Chem. Biol.* **2021**, *16*, 2244–2254. [[CrossRef](#)]
28. Ball, L.E.; Garland, D.L.; Crouch, R.K.; Schey, K.L. Post-translational Modifications of Aquaporin 0 (AQP0) in the Normal Human Lens: Spatial and Temporal Occurrence. *Biochemistry* **2004**, *43*, 9856–9865. [[CrossRef](#)]
29. Geiger, T.; Clarke, S. Deamidation, isomerization, and racemization at asparaginyl and aspartyl residues in peptides. Succinimide-linked reactions that contribute to protein degradation. *J. Biol. Chem.* **1987**, *262*, 785–794.

- 
30. Clarke, N.D. A proposed mechanism for the self-splicing of proteins. *Proc. Natl. Acad. Sci. USA* **1994**, *91*, 11084–11088. [[CrossRef](#)]
  31. Hains, P.G.; Truscott, R.J.W. Post-Translational Modifications in the Nuclear Region of Young, Aged, and Cataract Human Lenses. *J. Proteome Res.* **2007**, *6*, 3935–3943. [[CrossRef](#)] [[PubMed](#)]